Optical Prosperities of Ag–ZnO Composition Nanofilm Synthesized by Chemical Bath Deposition

Y.F. Wang[a], J.H. Yao[a,*], G. Jia[b] and H. Lei[a]

[a]The Key Lab of Advanced Technique and Fabrication for Weak-Light Nonlinear Photonics Materials Ministry of Education, TEDA Applied Physics School, Nankai University, Tianjin 300475, P.R. China

[b]Tianjin Institute of Urban Construction, Tianjin 300384, P.R. China

(Received June 10, 2010)

Ag–ZnO composite thin films were prepared on glass substrates by chemical bath deposition at lower temperature. The samples were characterized by X-ray diffraction, scanning electron microscopy, photoluminescence and the optical transmission spectra. The morphology analysis showed that Ag nanoparticles were not deposited on the ZnO nanorods surface but on the glass substrate. The influence of the reaction time on the size and density of Ag nanoparticles was studied, the results showed that the reaction time played an important role in determining of the optical characteristics. There were two obvious photoluminescence peaks located at about 395 nm and 471 nm, respectively. The blue emission centered at 471 nm can be ascribed to the electron transition from Zn_i to V_{Zn}.

PACS: 81.15.Lm, 78.66.Hf, 78.55.Et, 68.37.Hk

1. Introduction

Owing to its large exciton binding energy of 60 meV and wide band gap energy of 3.37 eV at room temperature, ZnO has attracted considerable attention as one of the most important promising optical-electron material. ZnO thin films have been used in transparent electrode [1], gas sensor [2], solar cells [3], room temperature UV laser [4], and so on. However, it is difficult to achieve visible light absorption on a single ZnO material. Many binary compounds such as CdS, CdSe have been used to deposit on the ZnO surface to enhance its ability of absorbing visible light. Jia et al. has even prepared the ternary CdZnS semiconductor film by chemical bath deposition (CBD) to study the absorption in the visible light [5, 6]. The Ag nanoparticles have been mostly extensively investigated as the important candidate for wide band gap material to absorb light. Ag nanoparticles can offer high performance absorption in visible light without any highly toxic elements. Many different methods have been used to prepare Ag–ZnO composite nanofilm, such as sonochemical synthesis [7], the RF magnetron sputtering method [8], sol–gel process [9], reduction method in aqueous solution [10], microwave radiation [11], and so on. However, there are few reports on the preparation of Ag–ZnO composite nanofilm on the glass substrate by CBD. It was an important method to synthesize nanofilms. The method is cost-effective, simple and can be carried out under low temperature.

In this paper, the simple CBD method was used to obtain the Ag–ZnO composite nanofilm on the glass substrate. Effects of Ag nanoparticles on the optical properties of ZnO nanorods films were investigated in detail. The forming mechanisms of Ag and ZnO were also further studied.

2. Experimental details

All chemicals used in this experiment, such as zinc acetate dihydrate $Zn(Ac)_2{\cdot}2H_2O$, hexamethylenetetramine ($C_6H_{12}N_4$), silver nitrate ($AgNO_3$), stannous dichloride dihydrate ($SnCl_2{\cdot}2H_2O$) and hydrochloric acid (35%) were analytical grade reagents and were used as purchased without further purification. The glass substrates were first immersed in a 3 mol/L sodium hydroxide solution for 3 h, and then washed by deionized water (DI), followed by ultrasonicating for 15 min, after that they were immersed in the mixed solution of hydrogen peroxide and concentrated sulfuric acid (1:3) for 10 h, washed by deionized water and ultrasonicating again, then dried in air. Before preparing the ZnO nanorods, the glasses were kept in a $SnCl_2$/HCl mixed solution for at least 1 h in order to show hydrophilic properties.

The experiment procedure was described as follows: the equimolar (1:1) mixed solution of zinc acetate dihydrate and hexamethylenetetramine was used. 0.5268 g $Zn(CH_3COO)_2 \cdot 2H_2O$ and 0.3365 g $C_6H_{12}N_4$ were first

* corresponding author; e-mail: yaojh@nankai.edu.cn

dissolved in 80 mL deionized water in a 100 mL beaker under mild magnet stirring for 5 min at room temperature. The pretreated glass substrate was then immersed in the solution at 90 ℃ for 1 h. The obtained ZnO film was washed with deionized water and dried in air. Next, 0.0082 g $AgNO_3$ and 0.3365 g $C_6H_{12}N_4$ were disolved in the 80 mL deionized water with stirring, and then the as-prepared ZnO films were immersed into the mixed solutions and the beakers were stored in the water bath at 95 ℃ for different time without any stirring. Then the substrates were rinsed with deionized water and dried in air before characterization.

The crystalline structure of the as-prepared Ag–ZnO composite nanofilms were characterized by X-ray diffraction (XRD) with a DX-2700 diffractometer using Cu K_α radiation (λ = 1.54178 Å). The diffraction angle was scanned from 20° to 80° at the scanning speed of 0.02° per second. The morphology and optical properties were studied by scanning electron microscopy (SEM) performed on SHIMADZU SS-550 microscope with 30 kV. PL spectroscopy was measured using Edinburgh FSP920 fluorescence spectrometer with the Xe lamp as the excitation light source and transmission spectra were observed with an UV/visible spectrophotometer with rated power 120 W and AC 220 V.

3. Results and discussion

We first consider the growth mechanism of Ag–ZnO composite thin film by CBD. The following chemical equations are involved in the reaction process:

$$(CH_2)_6N_4 + 6H_2O \leftrightarrow 6HCHO + 4NH_3\,, \quad (1)$$

$$NH_3 + H_2O \rightarrow NH_4^+ + OH^-, \quad (2)$$

$$Zn^{2+} + 2OH^- \rightarrow ZnO(\text{nuclei}) + H_2O\,, \quad (3)$$

$$Zn^{2+} + 4OH^- \rightarrow Zn(OH)_4^{2-}, \quad (4)$$

$$Zn(OH)_4^{2-} \rightarrow ZnO + H_2O + 2OH^-, \quad (5)$$

$$HCHO + 2Ag^+ + H_2O \rightarrow HCOOH + 2Ag + 2H^+. \quad (6)$$

As temperature elevates, the decomposition of zinc acetate dihydrate and hexamethylenetetramine accelerates and the concentration of Zn^{2+} and OH^- increases correspondingly (Eqs. (1) and (2)) [12, 13]. When the concentration of the Zn^{2+}, OH^- and $Zn(OH)_4^{2-}$ reaches a supersaturated degree, the process of rapid nucleation of ZnO starts (Eq. (3)) and ZnO nanostructures begin to generate (Eqs. (4) and (5)) in the reactive solution with an appropriate temperature [14], meanwhile, Ag^+ is reducted to be Ag nanoparticles by HCHO (Eq. (6)).

Figure 1 shows SEM images of as-prepared Ag–ZnO composite nanofilm deposited on glass substrate as the changing of the reaction time. The samples of ZnO nanorods were dipped in 0.6 mmol/L $AgNO_3$ solution, which were then aged at 95 ℃ for different time. A number of ZnO nanorods can be observed on the substrate and seem uniform with the length of about 2 μm and the average diameter of 300 nm. It can be obviously seen that Ag nanoparticles were not loaded on the ZnO nanorods surface even if increasing the reaction time but deposited on the glass substrate. The reason may be ascribed to the weak absorption between the ZnO nanorods surface and the Ag nanoparticles. Song et al. [10] successfully prepared ZnO/Ag composite microspheres, they dealed the ZnO microspheres with $SnCl_2{\cdot}2H_2O$ aqueous solution in order to sensitize and activate the surface of ZnO microspheres and the Ag nanoparticles were well coated on the ZnO surface. It can be noted that the size and density of Ag nanoparticles increased with the increase of the reaction time, which further improved that the Ag nanoparticles were formed in the solution, and then were deposited on the surface of glass.

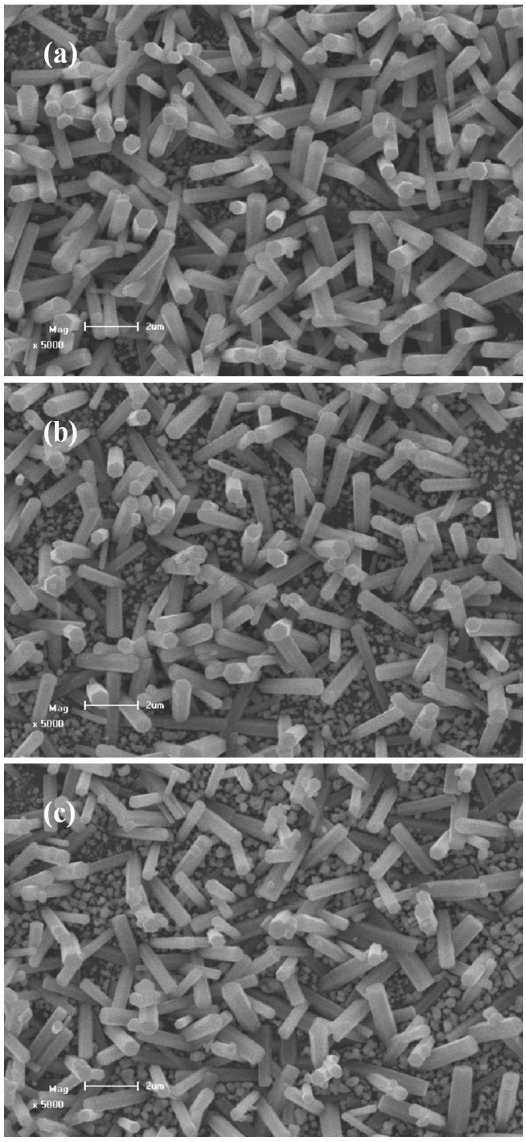

Fig. 1. SEM images of as-prepared Ag–ZnO composition nanofilm deposited on glass substrate with different reaction time (a) 3 h, (b) 4 h, (c) 5 h.

Figure 2 shows the XRD patterns of Ag–ZnO composite nanofilm deposited on the glass substrate with differ-

ent deposition time which were obtained by dipping the samples of ZnO nanorods in the solution of 0.6 mmol/L Ag^+ concentration. The diffraction peaks of ZnO are at $2\theta = 32.48°$, $35.15°$, $36.87°$, $48.29°$, $57.22°$, $63.54°$, $67.06°$, all those diffraction peaks are well indexed to the Bragg reflections of the standard wurtzite structure zinc oxide (JCPDS Card File No. 36-1451, $a = 0.3249$ nm and $c = 0.5206$ nm) [15] and correspond to (100), (002), (101), (102), (110), (103) and (112). In addition, the typical silver XRD peak (111) at about 38.82° is also observed. No peaks from any other phase of ZnO or impurity are identified. The corresponding lattice parameters of ZnO component were calculated and found the lattice constants little changing. The data suggested that silver atoms were not incorporated into the ZnO lattice. According to the Gaussian fitting of the Ag XRD peak (111), the size of Ag nanoparticles was calculated by the Scherrer formula. The calculation result shows that the size and density Ag nanoparticles increase with the increase of the reaction time. The results were in good agreement with the analysis of SEM observation.

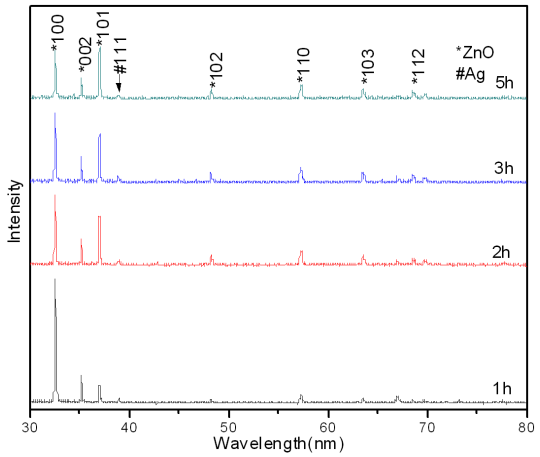

Fig. 2. XRD data of Ag–ZnO composite nanofilm synthesized by dipping the as-prepared ZnO nanorods on glass substrate in the solution of 0.6 mmol/L Ag^+ concentration and deposited at 95 °C with different deposition time.

Figure 3 shows the PL spectra of Ag–ZnO composite nanofilm at different deposition time with the excitation wavelength at 325 nm. Two obvious luminescence peaks are observed, the near-band-edge (NBE) emission band is from 370 to 430 nm and the central value is 395 nm, which is usually ascribed to the radiative recombination of ZnO free excitons [16]. Lin calculated the energy levels of the intrinsic defects in undoped ZnO films and figured out the energy levels draft of the intrinsic defects [17]. It also suggested that the blue emission centered at 471 nm (2.63 eV) may be due to the electron transition from Zn_i to V_{Zn}. The location of the UV emission centered at 395 nm does not change while its intensity has become stronger as the deposition time increases. A possible reason for the UV peak enhancement may be related to the surface plasmon resonance of silver nanoparticles [18]. When the interaction between the UV luminescence emitted from ZnO nanorods and silver nanoparticles has happened, there would be surface plasmon resonance so that the local crystalline field enhanced quickly, which further results in the increased intensity of the UV photoluminescence. As the deposition time increases, the number of silver nanoparticles becomes larger and surface plasmon resonance enhances, so the intensity of the UV photoluminescence peak enhances.

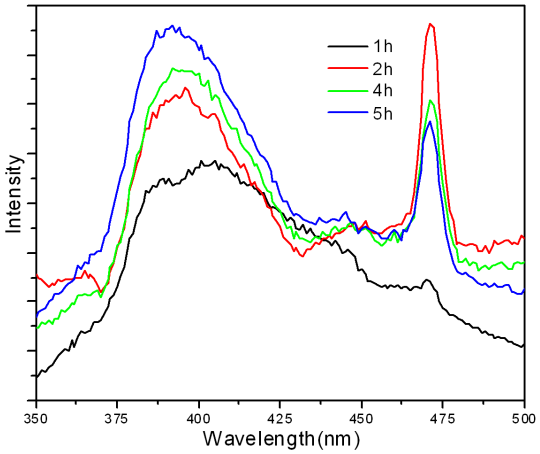

Fig. 3. The PL spectra at room temperature of Ag–ZnO nanofilms with different bath deposition time under the excitation wavelength at 325 nm.

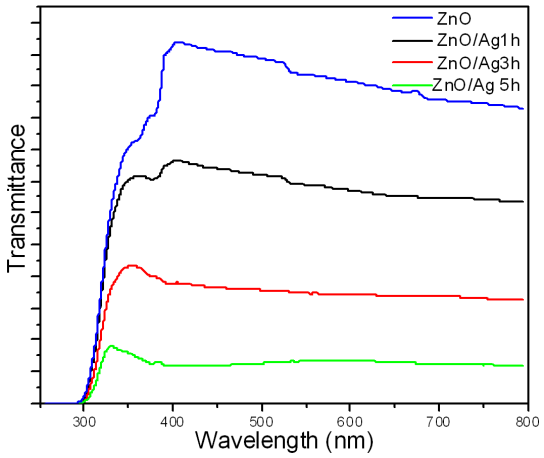

Fig. 4. Optical transmittance of Ag–ZnO composite nanofilm on the glass substrate with different deposition time.

Figure 4 shows the optical transmittance of undoped ZnO nanorods and Ag–ZnO composite deposited for different time in the wavelength range 200–800 nm. With increasing the deposition time, the transmittance obviously decreases and the absorption edge shifts slightly to a longer wavelength region. The red shift of the ab-

sorption peak should be due to the quantum-size effects for Ag.

4. Conclusions

In summary, a low-temperature route to obtain Ag–ZnO composite nanofilm has been presented. ZnO nanorods can be observed on the substrate with the length of about 2 μm and the average diameter of 300 nm. The SEM images suggested that Ag nanoparticles were not deposited on the ZnO surface but on the glass substrate. Two obvious photoluminescence peaks located at about 395 nm and 471 nm, respectively, were observed, as the increase of reaction time, the intensity of the NBE emission peak increases while that of the blue emission peak decreases, which is attributed to the surface Ag nanoparticles plasmon resonance.

Acknowledgments

This work has been supported in part by the Natural Science Foundation of Tianjin (09JCYBJC04100, 08JCYBJC14800), the Science and Technology Plan Projects of the Ministry of Construction of China (2008-K7-10), Chinese National Key Basic Research Special Fund (2010CB933801) and the National Natural Science Foundation of China (11074129).

References

[1] D.J.D. Moet, P. de Bruyn, P.W.M. Blom, *Appl. Phys. Lett.* **96**, 153504 (2010).

[2] S. Roy, S. Basu, *Bull. Mater. Sci.* **25**, 513 (2002).

[3] T.W. Hamann, A.B.F. Martinson, J.W. Elam, M.J. Pellin, J.T. Hupp, *Adv. Mater.* **20**, 1560 (2008).

[4] A. Ohtomo, M. Kawasaki, Y. Sakurai, Y. Yoshida, H. Koinuma, P. Yu, Z.K. Tang, G.K.L. Wong, Y. Segawa, *Mater. Sci. Eng. B* **54**, 24 (1998).

[5] G.Z. Jia, N. Wang, L. Gong, X.N. Fei, *Chalcogen. Lett.* **6**, 463 (2009).

[6] G.Z. Jia, N. Wang, L. Gong, X.N. Fei, *Chalcogen. Lett.* **7**, 377 (2010).

[7] F. Li, X.Q. Liu, Q.H. Qin, J.F. Wu, Z. Li, X.T. Huang, *Cryst. Res. Technol.* **44**, 1249 (2009).

[8] H.F. Lu, X.L. Xu, L. Lu, M.G. Gong, Y.S. Liu, *J. Phys., Condens. Matter* **20**, 472202 (2008).

[9] C.-S. Hong, H.-H. Park, H.-H. Park, H.-J. Chang, *J. Electroceram.* **22**, 353 (2009).

[10] W. Song, Y.F. Wang, H.L. Hu, B. Zhao, *J. Raman Spectrosc.* **38**, 1320 (2007).

[11] Sayan Bhattacharyya, A. Gedanken, *J. Phys. Chem. C* **112**, 659 (2008).

[12] Q. Ahsanulhaq, S.H. Kim, Y.B. Hahn, *J. Phys. Chem. Solids* **70**, 627 (2009).

[13] J. Tang, X.R. Yang, *Mater. Lett.* **60**, 3487 (2006).

[14] J.-H. Jang, J.-H. Park, S.-G. Oh, *J. Ceram. Proc. Res.* **10**, 783 (2009).

[15] O. Lupan, S. Shishiyanu, V. Ursaki, H. Khallaf, L. Chowb, T. Shishiyanu, V. Sontea, E. Monaico, S. Railean, *Solar Energy Mater. Solar Cells* **93**, 1417 (2009).

[16] Y. Feng, Y.X. Zhou, Y.Q. Liu, G.B. Zhang, X.Y. Zhang, *J. Lumin.* **119-120**, 233 (2006).

[17] B.X. Lin, Z.X. Fu, Y.B. Jia, *Appl. Phys. Lett.* **79**, 7 (2001).

[18] S.L. Smitha, K.M. Nissamudeen, Daizy Philip, K.G. Gopchandran, *Spectrochim. Acta A* **71**, 186 (2008).